

A deformation model for non-rigid registration of the kidney

Rowena E. Ong¹, Courtenay L. Glisson¹, S. Duke Herrell³, Michael I. Miga^{1,2}, Robert Galloway^{1,4}

¹Vanderbilt University, Department of Biomedical Engineering, Nashville, TN 37235

²Vanderbilt University, Department of Radiology and Radiological Sciences, Nashville, TN 37235

³Vanderbilt University, Department of Urologic Surgery, Nashville, TN 37235

⁴Vanderbilt University, Department of Neurosurgery, Nashville, TN 37235

{Rowena.Ong, Courtenay.L.Glisson, Duke.Herrell, Michael.I.Miga, Bob.Galloway}
@vanderbilt.edu

ABSTRACT

The development of an image-guided renal surgery system may aid tumor resection during partial nephrectomies. This system would require the registration of pre-operative kidney CT or MR scans to the physical kidney; however, the amount of non-rigid deformation occurring during surgery and whether it can be corrected for in an image-guided system is unknown. One possible source of non-rigid deformation is a change in pressure within the kidney: during surgery, clamping of the renal artery and vein results in a loss of perfusion, such that the subsequent cutting of the kidney and fluid outflow may cause a decrease in intrarenal pressure. In this work, we attempt to characterize the deformation due to cutting of the kidney and subsequent changes in intrarenal pressure. To accomplish this, we perfused a resected porcine kidney at a physiologically realistic pressure, clamped the renal vessels, and cut the kidney using a tracked scalpel. The resulting deformation was tracked in a CT scanner using 15-20 glass bead fiducials attached to the kidney surface. A modified form of Biot's consolidation model was used to simulate the deformation, and the accuracy was assessed by calculating the target registration error and image similarity.

Keywords: Modeling, biomechanics, finite element, consolidation, renal cell carcinoma, partial nephrectomy, clamping, kidney perfusion

1. INTRODUCTION

The American Cancer Society has estimated that over 54,000 new cases of renal cancer will be diagnosed and over 13,000 people will die of the disease in 2008 [1]. Surgery is usually the recommend treatment if the renal tumors are found before metastasis. Partial nephrectomies, in which only a portion of the kidney is removed, are usually recommended over full nephrectomies for small renal tumors. Recent studies [2, 3] have found that patients who undergo partial nephrectomies have about the same tumor re-occurrence and long-term survival rates as those who undergo radical nephrectomies; however, partial nephrectomy patients have the advantage of retaining greater renal function.

One challenge surgeons face during partial nephrectomies is the location of sub-surface tumor margins, small tumors deep inside the kidney, blood vessels, and other structures that may not be visible from the kidney surface. To facilitate the location and removal of tumors during partial nephrectomies, an image-guided surgery system may be helpful. By providing the surgeon a navigational aid, this system would ideally allow the surgeon to spare more healthy nephrons while still obtaining a clear tumor margin and avoiding critical vessels. Image-guided renal systems are currently being developed that utilize pre-operative and intra-operative imaging to provide an interactive display of the kidney. These systems generally require the registration of pre-operative and intra-operative images to the physical kidney and the tracking of surgical tools. Much work has been done previously to develop image-guided surgery systems for the brain, liver, and other organs [4][5][6].

Ideally, an image-guided renal surgery system would not only account for changes in kidney position and orientation by performing a rigid alignment, but also for changes in kidney shape that occur during surgery. This non-rigid deformation may be caused by external forces applied to the kidney (e.g. by surgical tools, retractors, laparoscopic insufflation), by physiological changes, or by other surgical conditions. One surgical condition that may cause non-rigid kidney deformation is the clamping of the renal vessels. During partial nephrectomies, the renal artery and vein are often clamped, causing a loss of perfusion. The subsequent cutting of the kidney during surgery causes blood and fluid loss, which decreases intrarenal pressure, inducing a loss of turgor and general shrinkage of the kidney. The extent of the deformation caused by intrarenal pressure decreases and whether it can be corrected for in an image-guided surgical system is not well known.

In our previous work [7], we found that resected human kidneys experienced a mean shift of about 3 mm when subjected to clamping and unclamping; however, the decrease in perfusion pressure and an incision to the parenchyma was not controlled for. In this work, we attempt to measure and model the deformation that occurs when a kidney under a controlled renal arterial pressure is subject to a parenchymal incision. In addition, the kidney deformation model described earlier is refined to incorporate more realistic renal structures and assess its error. In the future, we hope to utilize the model in a non-rigid registration to correct for intra-operative kidney deformation in an image-guided renal surgery system.

2. METHODS

2.1 Experiments

To track the kidney deformation that occurs when the renal vessels are clamped and a parenchymal incision is made, the following procedure was followed:

1. Three anesthetized pigs were heparinized to prevent blood clots and euthanized. The six porcine kidneys were then resected.
2. Between 10-20 glass bead fiducials 2 mm in diameter were attached to each kidney surface, and the kidneys were fixed to their enclosing containers in order to eliminate any rigid motion.
3. The kidneys were perfused with saline at a renal arterial pressure of 100mmHg, a physiologically reasonable pressure. To this end, the renal artery and vein of the resected porcine kidneys were cannulated with tubing 1-3mm in diameter, and the tubing was sutured to the vessels to keep it from slipping out. The tubing was connected to 1000mL intravenous saline bags and primed before attachment to the renal vessels. The saline IV bags were hung 1.36 m above the kidney to induce a renal arterial pressure of 100mmHg. The saline was allowed to flow for a few minutes so that equilibrium could be reached.
4. The renal artery and vein were clamped.
5. A pre-deformation CT image of each kidney was taken (90 KeV, 300 mAs, 0.8 mm slice thickness). The kidney container was clamped to the CT table to eliminate any rigid motion.
6. A scalpel whose tip was tracked by a Polaris Spectra (Northern Digital Inc., Ontario, Canada) infrared tracking device was used to make an incision in the renal parenchyma. Blood and fluid were allowed to drain from the incision site. A Polaris target attached to the handle of the scalpel (Figure 1), and a prior calibration allowed the scalpel tip to be localized. To enable the registration of the scalpel coordinates to the kidney/CT image space, 6-8 glass bead fiducials 5mm in diameter were glued to the kidney container and localized using a Polaris probe.
7. A post-deformation CT image of the kidney was taken. As the kidney container was clamped to the CT table, the post- and pre-deformation images should be in the same coordinate space and no rigid registration should be necessary.

To measure the amount of deformation, the 2mm glass fiducials were localized in the pre- and post-deformation CT images by calculating the intensity-based centroids. The mean shift at the surface fiducials was then calculated for the six kidneys. The tracked scalpel was rigidly registered to the CT image space using the six glass fiducials glued to the kidney container.

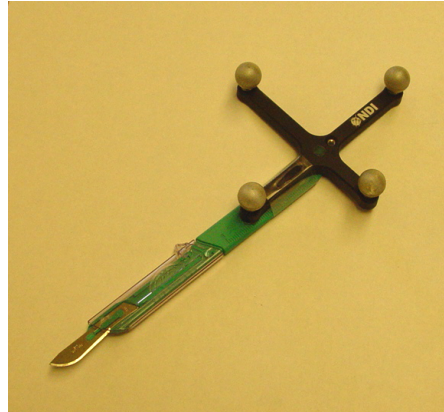


Figure 1. Scalpel with Polaris target attached to handle, used to track an incision made to the renal parenchyma.



Figure 2. Porcine kidney with glass bead fiducials attached to the surface to track deformation. The kidney was perfused with saline and cut with tracked scalpel.

2.2 Model

Although little data is available for the biomechanical properties of the human kidney some work has been [8,9] performed to determine the material properties of animal kidneys. Material testing on excised porcine kidney tissue [8] indicates that the cortex and medulla display nonlinear, anisotropic elastic behavior under uniaxial compression. The parenchyma in the radial direction (the directions along which the tubules are aligned) was found to be less stiff than in the cross-tubule directions. Additionally, the response of the tissue under uniaxial compression was considered nonlinear and was characterized by a compliant, linear portion up to about 5% strain, followed by a stiffening, nonlinear response. Based on these studies and our observation that clamping and cutting of the kidney does not produce strains greater than 5-10%, we have chosen a linear elastic model that accounts for the drainage of fluid and anisotropic structure.

The kidney deformation due to clamping of the renal artery and vein was modeled based on consolidation theory, which describes the behavior of a porous, sponge-like material and has been used in previous soft tissue deformation models [6]. A modified form of the porous-media model was used, and the equations describing kidney deformation were chosen to be

$$\nabla \cdot \sigma = \nabla P \quad (1)$$

$$\nabla \cdot (-K \nabla P) = \kappa_c (P_i - P) \quad (2)$$

where σ is the mechanical stress tensor, P is the general tissue pressure associated with the turgor of the kidney in its homeostatic condition, P_i is the interstitial hydrostatic pressure, κ_c is the hydraulic permeability, and K is the hydraulic conductivity tensor. The kidney tissue was assumed to be a linear elastic, isotropic, homogeneous tissue, and the mechanical stress σ was describing using Hooke's law.

The boundary conditions were set as follows: the bottom surface of the kidney and hilum area were fixed with no change in pressure normal to the surface ($dP/dN = 0$), the incision was set as stress-free and drainage area ($P=0$), and the remaining surface was set as stress-free with $dP/dN = 0$. The hydraulic conductivity tensor was set to simulate the anisotropic drainage due to the pyramidal structure of the renal tubules.

In addition, the porous media model was compared to a linear elastic model and linear elastic anisotropic model. The boundary conditions were set as follows: the bottom surface and hilum area of the kidney were fixed, a type 2 surface force of 70 Pa in the outward normal direction was applied at the incision, and a type 2 surface force of 1000 Pa was applied in the direction of gravity to simulate the loss of turgor due to loss of intrarenal pressure. For the anisotropic model, the properties shown in Table 1 were used. The isotropic model parameters were set as follows: Young's modulus $E=8300$ Pa, Poisson's ratio $\nu=0.45$. All three models were solved in three Cartesian dimensions using the Galerkin finite element method and Lagrange polynomial weighting functions.

The directions of the renal tubules, from which the anisotropic directions were obtained, were generated by the following method: the approximate medial axis was found, and for each mesh node, the closest point on the medial axis was found. Thus the shortest vectors connecting each mesh node with the medial axis were found and assigned as the directions of anisotropy. See Figure 3 for an illustration of the medial axis and generated renal tubule directions.

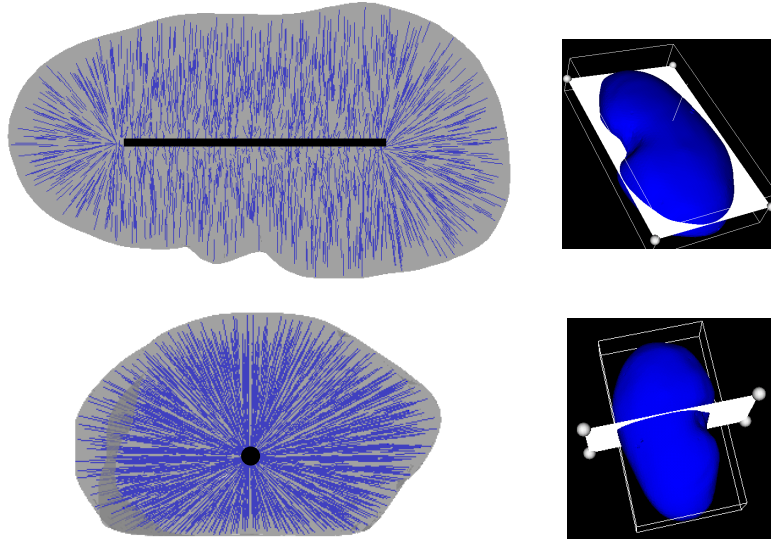


Figure 3. Two orthogonal views of pig kidney, with simulated renal tubules displayed by blue vectors. The thick black line indicates the medial axis from which the renal tubules were generated.

Table 1. Anisotropic linear elastic model parameters: Young's modulus (E) and Poisson's ratio (Nu) for longitudinal (L) and transverse (T) directions and shear modulus (G).

E_L (Pa)	E_T (Pa)	Nu_L	Nu_T	G
10000	5000	0.4	0.2	2083.33

2.3 Validation

The CT image volumes were segmented, three-dimensional finite element meshes were generated, the mesh was split to simulate the tracked incision, and the model was used to predict deformation for the third pig kidney. The target registration error was calculated as the average distance between the true displaced fiducial locations (found in the post-deformation image) and those predicted by the model. The magnitude error was calculated as the difference between the magnitudes of the true displacement vectors and those predicted by the model.

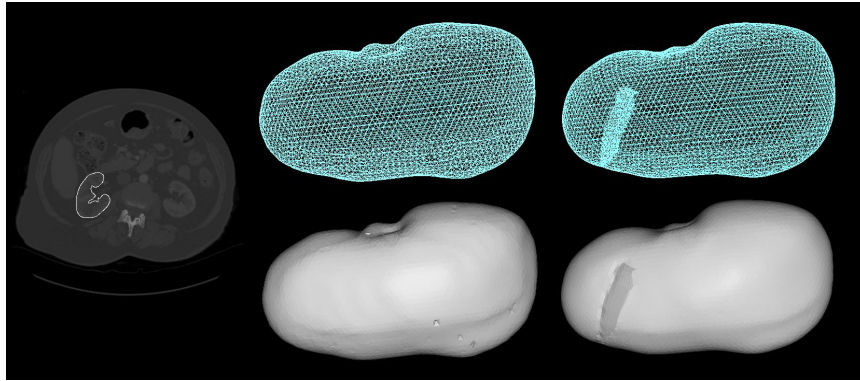


Figure 4. Segmented CT slice (left), 3D kidney mesh (middle), 3D kidney mesh split along tracked incision (right).

3. RESULTS

3.1 Deformation Measurement

The amount of deformation that occurred when six pig kidneys were perfused at 100mmHg, clamped, and then cut with a scalpel is shown in Table 2. The displacements measured at the surface fiducials localized in the pre- and post-deformation images was found to be between 3-6 mm. The mean deformation for all six kidneys was 4.4 mm. The magnitudes of the displacements as distributed across the surface of the kidney can be seen in Figure 5. Here we observed that the displacement magnitudes in general decrease with increased distance from the incision.

Table 2. Amount of deformation that occurred when six pig kidneys were perfused at 100mmHg, clamped, and then cut with a scalpel. Displacement was tracked using glass fiducials, localized from pre- and post-deformation CT images, and the mean shift at these surface fiducials was then calculated.

Kidney	Displacement at surface fiducials (mm)		
	Mean	Std dev	Max
1	4.7	2.2	9.2
2	3.4	2.0	7.4
3	6.7	2.4	11.4
4	4.5	2.2	7.2
5	3.8	1.7	6.1
6	3.4	1.8	5.7
Mean	4.4		

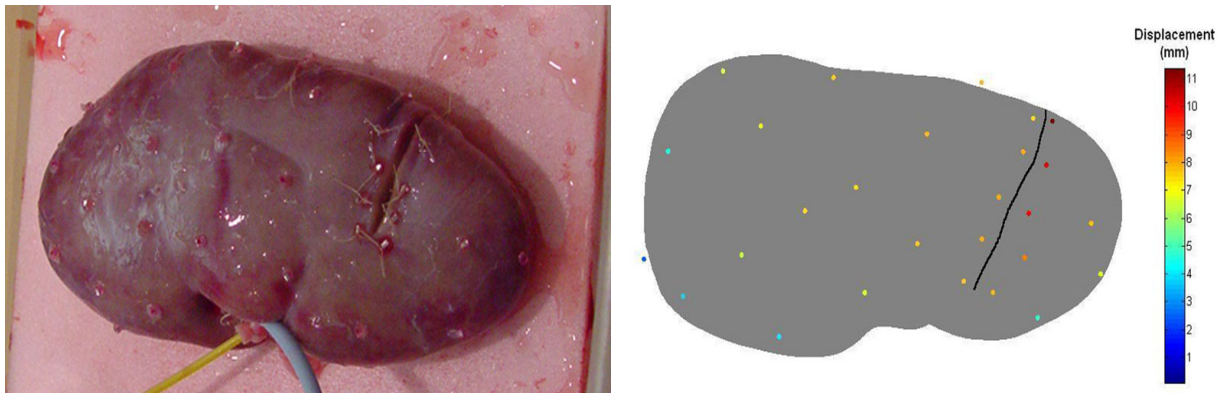


Figure 5. Left: Photograph of pig kidney 6 post-incision. Fiducials attached to the surface can be seen. Right: Fiducial locations color-coded by absolute distance change.

3.2 Model Validation

The general pattern of deformation predicted by the anisotropic linear elastic model is shown in Figure 6, which displays the signed closest distance between the pre- and post-deformation meshes. A negative distance in this case indicates an area where the post-deformed mesh is located inside the pre-deformed mesh, and a positive distance where the post-deformed is outside the pre-deformed mesh. Here we see the model predicts a general “sinking in” of the kidney surface in the direction of gravity (indicated by the blue areas), and a small expansion along the lateral edges (indicated by the green).

Figure 7 displays the model-predicted and true displacement vectors. The TRE and magnitude error for two simulations is shown in Table 3. The anisotropic linear elastic model performed the best, but only slightly better than the linear elastic model. The porous media model incorporating an anisotropic hydraulic conductivity tensor had much higher TRE and magnitude errors.

Table 3. TRE and magnitude error for linear elastic and anisotropic linear elastic models for kidney 3.

	TRE (mm)			Magitude error (mm)		
	Mean	Median	Max	Mean	Median	Max
Linear elastic model	3.4	3.3	6.5	1.6	1.6	5.3
Anisotropic linear elastic	3.2	3.0	6.2	1.6	1.2	4.9

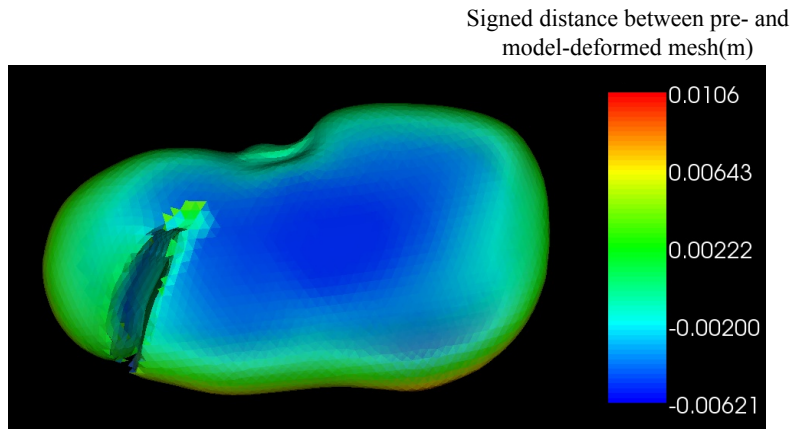


Figure 6. Mesh deformed by anisotropic linear elastic model, where color represents the signed distance between the pre-deformation and model-deformed meshes for kidney 3. Negative distances represent where model-deformed mesh has receded and positive distances where the mesh has expanded.

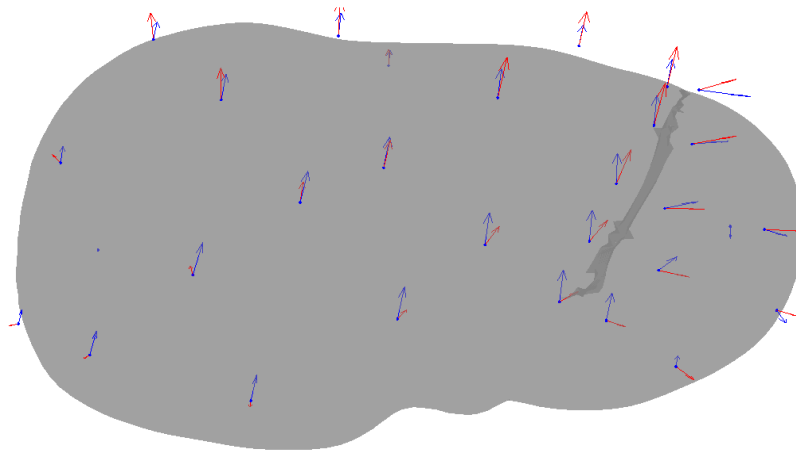


Figure 7. Pre-deformation mesh for kidney 3 with blue arrows representing true displacements and red arrows representing displacements predicted by the anisotropic linear elastic model.

4. DISCUSSION

The experimental data obtained give us a general estimate of the amount of deformation that can be expected when an incision is made in the parenchyma of a clamped kidney. The average amount of displacement for six pig kidneys was found to be between 3-6mm. This work improves upon the preliminary results found in our previous paper [7] by controlling for the initial renal arterial pressure and accounting for parenchymal incisions.

In addition to measuring the deformation, the pattern of displacement vectors across the surface of the kidney was analyzed. Eigenvector analysis of displacement vectors at the fiducials shows that the absolute location changes primarily in one direction, that is, downward in the direction of gravity as the kidney loses turgor. (The dominant eigenvector is approximately five times larger than the next largest one). This effect seems to be primarily caused by the loss of fluid and pressure within the kidney. Analysis of the fiducial locations on either side of the incision line is also useful. The fiducials on either side of the incision shows the incision opening as you would suspect. From the origin of the incision to its termination for kidney 3, relative spacing of fiducials spanning the incision goes from 0.7 mm to 3.3 mm to 5.9 mm to 8.1 mm. So the incision opening widens from the origin to the point of termination. Finally, the displacements seem to decrease in magnitude as the distance from the incision increases. One hypothesis that could explain this pattern is that the displacement magnitudes could be proportional to amount of drainage in that area. Therefore, it would make sense that greater displacements might be seen in the areas closer to the incision than farther away, as there might be more drainage in that area.

The preliminary model results show that about 50% of the kidney shift can be corrected for using a model. The anisotropy of the kidney due to the structure of the renal pyramids was incorporated and seemed to make a small amount improvement over the isotropic model; however, whether the improvement is significant is still to be determined. Further improvements to the model might result from incorporating the differences in the renal capsule, medulla, cortex, and renal pelvis material properties. Also, as the direction of the renal tubules in this study was simulated, greater model accuracy might be obtained if kidney-specific renal tubule directions could be obtained. Possibly diffusion tensor imaging could be used to obtain a more accurate estimate of the renal tubule directions.

Future work includes improving the model and exploring methods to address the extensive computational challenges associated with incorporating a model-based correction into an image-guided system. Possibly, an atlas-based or GPU computing method may be used. In addition, studies are being planned to explore the effects of clamping and incisions in both ex-vivo perfused human kidneys and in-vivo human kidneys during surgery.

5. CONCLUSION

In this work, we measure and attempt to model the deformation that occurs when a clamped kidney loses fluid and turgor due to a parenchymal incision. The average amount of deformation was found to be 3-6mm, and the deformation appeared to have a principal component downward in the direction of gravity. The incision appeared to account for the remaining lateral components of the deformation. Preliminary model results show that about 50% of the non-rigid deformation can be corrected using a model. Incorporating the anisotropic structure of the renal pyramids seemed to give slightly less error; however, the improvement may not be significant. Future work includes improving the model, perhaps by incorporating the differences between renal capsule, medulla, cortex, and renal pelvis material properties. In addition, studies to explore the deformation in human kidneys are being planned.

ACKNOWLEDGEMENTS

The authors would like to thank Dr. Prashanth Dumpuri and Dr. David Kwartowitz for their help in experimental design and modelling; Dr. Phil Williams, Ms. Amy Nunnally, and Ms. Jamie Adcock in the Animal Care Dept. for their generous help and donation of resources for our experiments; Dr. Paul Milhoua, Dr. Hernan Altamar, Ms. Kathy Deal, and the staff of the Urologic Surgery Dept; and the Vanderbilt CT Department. This work was funded in part by a grant from Pathfinder Therapeutics, Inc.

REFERENCES

- [1] American Cancer Society. 2007. "Cancer Facts and Figures." www.cancer.org.
- [2] Becker, F., Siemer, S., Humke, U., et al. "Elective nephron sparing surgery should become standard treatment for small unilateral renal cell carcinoma: Long-term survival data of 216 patients." *Eur Urol.* 49(2), 308-13 (2006).
- [3] Lau, W.K., Blute, M.L., Weaver, A.L., Torres, V.E., Zincke, H. "Matched comparison of radical nephrectomy vs nephron-sparing surgery in patients with unilateral renal cell carcinoma and a normal contralateral kidney." *Mayo Clin Proc.* 75(12), 1236-42 (2000).
- [4] Benincasa, A.B., Clements, L.W., Herrel, S.D., Chang, S.S., Cookson, M. S., Galloway R. L. "Feasibility study for image guided kidney surgery: assessment of required intraoperative surface for accurate image to physical space registrations." *Proc. of SPIE* 6141, 61411U (2006).
- [5] Dumpuri, P., Thompson, R. C., Dawant, B. M., Cao, A., Miga, M. I. "An atlas-based method to compensate for brain shift: Preliminary results." *Medical Image Analysis* 11(2),128-145 (2007).
- [6] Miga, M.I., Cash, D. M., Cao, Z., Galloway, R. L., Dawant, B., Chapman, W. C. "Intraoperative registration of the liver for image-guided surgery using laser range scanning and deformable models." *Proc. of SPIE* 5029, 350-359 (2003).
- [7] Ong, R. E., Herrell, S. D., Miga, M. I., Galloway, R. L. "A kidney deformation model for use in non-rigid registration during image-guided surgery," *Proc. of SPIE: Medical Imaging* (2008).
- [8] Farshad, M., Barbezat, M., Flueler, P., Schmidlin, F., Graber, P., Niederer, P. "Material characterization of the pig kidney in relation with the biomechanical analysis of renal trauma." *J Biomech.* 32(4), 417-425 (1999).
- [9] Miller, K. "Constitutive modeling of abdominal organs." *Journal of Biomechanics.* 33, 367-373 (2000).